

Article

Not peer-reviewed version

---

# Determination of the Hubble Constant and Sound Horizon from DESI Year 1 and DES Year 6 BAO Measurements and Low Redshift Data

---

[Jose Agustin Lozano Torres](#) \*

Posted Date: 31 May 2024

doi: 10.20944/preprints202405.2125.v1

Keywords: Hubble constant; sound horizon; cosmological parameters; numerical methods




Preprints.org is a free multidiscipline platform providing preprint service that is dedicated to making early versions of research outputs permanently available and citable. Preprints posted at Preprints.org appear in Web of Science, Crossref, Google Scholar, Scilit, Europe PMC.

Copyright: This is an open access article distributed under the Creative Commons Attribution License which permits unrestricted use, distribution, and reproduction in any medium, provided the original work is properly cited.

## Article

# Determination of the Hubble Constant and Sound Horizon from DESI Year 1 and DES Year 6 BAO Measurements and Low Redshift Data

Jose Agustin Lozano Torres <sup>1,2,\*</sup> 

<sup>1</sup> Instituto de Física, Universidad Nacional Autónoma de México, Ciudad de México 04510, México; jalozanotorres@gmail.com

<sup>2</sup> Instituto de Astronomía, Universidad Nacional Autónoma de México, Ciudad de México 04510, México;

**Abstract:** We perform new measurements of the expansion rate and the sound horizon at the end of the baryon decoupling and derive constraints on cosmic key parameters in the framework of the  $\Lambda$ CDM model, flat  $w$ CDM model, the  $\Lambda$ CDM+ $\Omega_K$  model and the phenomenological emergent dark energy (PEDE) model. We keep  $r_d$  and  $H_0$  completely free and use the recent dark energy spectroscopic instrument (DESI) Year 1 and dark energy survey (DES) Year 6 BAO measurements in the effective redshift range  $0.3 < z < 2.33$  combined with the compressed form of the Pantheon sample of Type Ia supernovae, the latest 33 observational  $H(z)$  measurements based on the differential age method, and the recent  $H_0$  measurement from SH0ES 2022 as an additional Gaussian prior. Combining BAO data with the observational  $H(z)$  measurements, and the Pantheon SNe Ia data, we get  $H_0 = 69.65 \pm 1.07 \text{ km s}^{-1} \text{ Mpc}^{-1}$ ,  $r_d = 147.71 \pm 2.18 \text{ Mpc}$  in  $\Lambda$ CDM model,  $H_0 = 70.06 \pm 1.07 \text{ km s}^{-1} \text{ Mpc}^{-1}$ ,  $r_d = 147.39 \pm 2.50 \text{ Mpc}$  in PEDE model. The spatial curvature is  $\Omega_k = 0.025 \pm 0.026$  and the dark energy equation of state is  $w = -1.016 \pm 0.056$ , consistent with a cosmological constant. We apply the Akaike information and the Bayesian information criterion test to compare the four models, and see that PEDE model performs better.

**Keywords:** hubble constant; sound horizon; cosmological parameters; numerical methods

## 1. Introduction

Observational experiments [1,2] have provided precise estimates of the key parameters of the standard cosmological model  $\Lambda$ CDM. Early measurements [1] estimated the value of the Hubble constant at  $H_0 = 67.4 \pm 0.5 \text{ km s}^{-1} \text{ Mpc}^{-1}$  with an uncertainty of less than  $1 \text{ km s}^{-1} \text{ Mpc}^{-1}$ . However, measurements in our local neighborhood of the Hubble constant [3–7] have been improved through the use of cepheid stars in a distance ladder method, leading to a more precise measurement of  $H_0$  as  $H_0 = 73.04 \pm 1.04 \text{ km s}^{-1} \text{ Mpc}^{-1}$  [7]. Despite the success of the  $\Lambda$ CDM model in of explaining the current Universe, the measurements of late-time [7] and early-time accelerated cosmic expansion [1] are in tension, with a discrepancy of  $4\sigma$ – $5.7\sigma$ . This tension suggests that either the measurements have systematic and calibration issues, or the standard cosmological model needs to be extended with new physics. As a result, various alternative cosmological models have been proposed to address the inconsistencies between cosmological surveys [8–20]. In the opposite directions, many observational studies have been made to provide estimates of the Hubble constant. such as quasar lensing [21,22], gravitational-wave events [23–25], fast radio bursts (FRBs) [26,27], Megamaser [28–30], red giant branch tip method (TRGs) [31–33], BAOs [34], etc [35]. Novel measurements of the Hubble constant independent of the CMB surveys and distance ladder measurements have been done. A dark siren measurement of the Hubble constant with the LIGO/Virgo gravitational wave event GW190412 and DESI galaxies combined with the bright standard siren measurement from GW170817 estimates  $H_0 = 77.96^{+23.0}_{-5.03} \text{ km s}^{-1} \text{ Mpc}^{-1}$  [36]. DECam Local Volume Exploration Survey (DELVE) analyses combined with gravitational wave events from the first three LIGO/Virgo observing runs estimates  $H_0 = 68.84^{+15.51}_{-7.74} \text{ km s}^{-1} \text{ Mpc}^{-1}$  [37]. Speaking of baryon acoustic oscillations (BAOs),

whose measurements from the dark energy spectroscopic instrument (DESI) and the dark energy survey (DES) play a key role in our analysis, they are sound waves traveling in the primordial plasma, frozen at the recombination epoch. The BAOs surveys give measurement results in terms of  $D_A(z)/r_d$ ,  $D_V(z)/r_d$ ,  $D_M(z)/r_d$ ,  $D_H/r_d$ , and  $H(z) \cdot r_d$ , where  $r_d$  is the sound horizon distance at the drag epoch. The baryons do not sense the dragging effect of photons until  $z_d \approx 1060$ , which sets the standard ruler for the BAOs. The Hubble constant  $H_0$  and the sound horizon  $r_d$  are strongly related, forming the so-called  $H_0 - r_d$  plane, linking the early- and late-time universe. In general,  $r_d$  is subject to the conditions of the early universe, hence constrained via early observations performed by Planck 2018 [1]. Instead of the calibration of  $r_d$  via early observations as per Planck, an alternative method is to combine BAO measurements with other low redshift observations.

In this work, we present the constraints of cosmological key parameters highlighting measurements of the Hubble constant  $H_0$  and the cosmic sound horizon at the baryon decoupling  $r_d$ , where we set the characteristic scale  $r_d$  of BAO as a free parameter in the framework of different cosmologies. Without regarding any assumption of the early time physics, we combine the measurement of baryon acoustic oscillations (BAO) in galaxy, quasar, and Lyman- $\alpha$  forest tracers for the first year of observations from the Dark Energy Spectroscopic Instrument (DESI) [38], the BAO measurement for the 6 year of observations from the Dark Energy Survey (DES) [39], the SNe-Ia Pantheon compilation data [40], the observational  $H(z)$  data (OHD), and the latest measurement of the Hubble constant done by SH0ES 2022 as an additional Gaussian prior [7]. The paper is structured as follows: Section 2 presents the cosmological models under study where will set constraints on cosmic key parameters. Section 3 summarizes our data and methodology. Results on cosmological parameters and constraints are given in Section 4. Finally, we present our discussion and conclusion in Section 5.

## 2. Theoretical Background

### 2.1. Flat $\Lambda$ CDM Model

The  $\Lambda$  cold dark matter ( $\Lambda$ CDM) model takes the dark energy equation of state (EoS) as the cosmological constant  $\Lambda$  with  $w = -1$ , acting as a negative pressure to counteract the effect of gravity. The Friedmann equation for this model is expressed as

$$E^2(z) = \Omega_r(1+z)^4 + \Omega_m(1+z)^3 + \Omega_{DE}(z), \quad (1)$$

where we can set  $\Omega_{DE}(z) = \Omega_\Lambda$ , with EOS  $w = -1$ . The Friedmann equation (1) depends on the free parameters  $\Omega_r$ ,  $\Omega_m$ ,  $\Omega_\Lambda$ . The term  $E(z)$  is the expansion rate and is the ratio  $H(z)/H_0$ , where  $H(z) = \dot{a}/a$  is the Hubble parameter at redshift  $z$  and  $H_0$  is the Hubble constant measured at present time.

### 2.2. $\Lambda$ CDM model with free spatial curvature

In the  $\Lambda$ CDM model, we depart from the assumption of spatial flatness by introducing a variable curvature parameter  $\Omega_K$ . In the framework of an FRW background, this is analogous to allowing the dark energy density  $\Omega_{DE} = 1 - \Omega_m - \Omega_K$  to vary independently from the matter density  $\Omega_m$ , while maintaining a constant dark-energy equation of state with  $w = -1$ . The Friedmann equation for this model is expressed as

$$E^2(z) = \Omega_r(1+z)^4 + \Omega_m(1+z)^3 + \Omega_K(1+z)^2 + \Omega_{DE}(z). \quad (2)$$

### 2.3. Flat Constant $w$ CDM model

The cosmological model  $w$ CDM assumes a constant EoS  $w$ . The Friedmann equation for  $w$ CDM model is expressed as

$$E^2(z) = \Omega_r(1+z)^4 + \Omega_m(1+z)^3 + \Omega_{DE}(1+z)^{3(1+w(z))}, \quad (3)$$

where Equation (3) depends on the free parameters  $\Omega_r$ ,  $\Omega_m$ ,  $\Omega_\Lambda$ , and  $w(z)$ . Despite the success of the cosmological constant fitting existing data very well, the small value of  $\Lambda$  relative to the theoretical estimations based on particle physics poses a conflict. This requires going beyond  $\Lambda$ CDM where dark energy has dynamics - time dependence, hence proposing cosmological models with dark energy equation-of-state parameterized.

### 2.4. Phenomenological Emergent Dark Energy (PEDE) Model

Generally, the parametrization of a given dark energy equation-of-state  $w$  can be a function of redshift  $z$  or the scale factor  $a(t)$  of the Friedmann-Lemaître-Robertson-Walker metric universe, noticing that  $1+z = a_0/a(t)$ , where  $a_0$  is the present value of the scale factor. Here, we consider a dynamical dark energy equation-of-state  $w$  parametrization called the phenomenological emergent dark energy (PEDE-CDM) model [51]. This model introduces a dark energy density written as

$$\Omega_{DE}(z) = \Omega_{DE} \times [1 - \tanh(\log_{10}(1+z))], \quad (4)$$

where  $\Omega_{DE} = 1 - \Omega_m - \Omega_r$ . From the PEDE model, we can write the Friedmann equation in terms of the expansion function as

$$E^2(z) = \Omega_r(1+z)^4 + \Omega_m(1+z)^3 + \Omega_{DE} \times [1 - \tanh(\log_{10}(1+z))] \quad (5)$$

where Equation (5) depend on free parameters  $\Omega_r$ ,  $\Omega_m$ ,  $\Omega_{DE}$ . This dark energy model with zero degrees of freedom as the  $\Lambda$ CDM model acts with no presence in early times, and emerges at later times.

## 3. Data and Methodology

In order to estimate and place constraints on the cosmological key parameters in the framework of different cosmologies that we have described above, we use the following observational data sets: the recent BAO measurements done by DESI year 1, DES year 6, observational  $H(z)$  data (OHD), the Pantheon Sample, and the local measurement of the Hubble constant  $H_0$  labelled as R22.

BAO measurements depend on the sound horizon at the epoch of baryon decoupling  $r_d$  at  $z_d \approx 1060$  in the standard model. It is given by

$$r_d = \frac{1}{H_0} \int_{z_d}^{\infty} \frac{c_s(z)}{E(z)} dz, \quad (6)$$

where the sound speed  $c_s(z)$  is a function of the baryon to photon densities ratio, and  $E(z)$  is the expansion rate function in terms of our present-day density fraction  $\Omega_r$ ,  $\Omega_m$ ,  $\Omega_{DE}$ , and  $\Omega_k$ . The sound horizon  $r_d$  is the characteristic scale to calibrate BAO observations, where it is often settled a prior of the CMB measurement. In this analysis, we remove the prior  $r_d$  from CMB Planck satellite and set  $r_d$  as a free parameter. The BAO measurements from surveys of galaxies, quasars and Lyman- $\alpha$  forest are given by the observables  $D_M(z)/r_d$ ,  $D_V(z)/r_d$ , and  $D_H(z)/r_d$ . The transverse comoving distance

$D_M(z)$  and the volume angle-average length  $D_V(z)$  that quantifies the average of distances measured along are linked to the expansion rate function  $E(z)$  by

$$D_M = \frac{c}{H_0} \int_0^z \frac{dz'}{E(z')}, \quad (7)$$

$$D_V(z) = [zD_H(z)D_M^2(z)]^{1/3}. \quad (8)$$

We use the recent BAO measurements from DESI year 1 data release (DESI DR1) and DES year 6 (DESY6) result which are performed at a series of redshifts, allowing constrains on the cosmic key parameters. The DESI DR1 and DESY6 BAO data points are listed in Table 1 with their corresponding redshifts  $z_{eff}$ , observables, measurements, and errors

**Table 1.** We present the recent 13 BAO measurements from the Dark Energy Spectroscopic Instrument (DESI) year 1 data release and Dark Energy Survey (DES) year 6 on which we perform our analysis.

$z_{eff}$	Observable	Measurement	Error	Year	Dataset Survey	Reference
0.30	$D_V/r_d$	7.92	0.15	2024	DESI BGS	[38]
0.51	$D_M/r_d$	13.62	0.25	2024	DESI LRG	[38]
0.51	$D_H/r_d$	20.98	0.61	2024	DESI LRG	[38]
0.71	$D_M/r_d$	16.84	0.32	2024	DESI LRG	[38]
0.71	$D_H/r_d$	20.08	0.60	2024	DESI LRG	[38]
0.85	$D_M/r_d$	19.51	0.41	2024	DES Year 6	[39]
0.93	$D_M/r_d$	21.73	0.28	2024	DESI LRG+ELG	[38]
0.93	$D_H/r_d$	17.87	0.35	2024	DESI LRG+ELG	[38]
1.32	$D_M/r_d$	27.80	0.69	2024	DESI ELG	[38]
1.32	$D_H/r_d$	13.82	0.42	2024	DESI ELG	[38]
1.49	$D_V/r_d$	26.09	0.67	2024	DESI QSO	[38]
2.33	$D_M/r_d$	39.71	0.94	2024	DESI Ly $\alpha$ QSO	[38]
2.33	$D_H/r_d$	8.52	0.17	2024	DESI Ly $\alpha$ QSO	[38]

In this analysis, we do not take into account the OHD obtained from the measurement of BAO. We only make use of the OHD from differential age method proposed in Ref. [55]. Table 2 shows an updated compilation of OHD covering a total of 33 data points given by the differential age method [55]. We also make use of the Pantheon compilation of 1048 SNe Ia in the redshift range  $0.01 < z < 2.3$  [40] and the Hubble constant estimation from the SH0ES team yielding to the Gaussian prior  $H_0 = 73.04 \pm 1.04 \text{ km s}^{-1} \text{ Mpc}^{-1}$  at 68% CL (R22) [7]. To extract constraints of our different cosmological scenarios, we implemented a nested sampling algorithm tailored for high-dimensional parameter space called *Polychord* developed by [41] to perform the calculations as done in [56,57].



**Table 2.** The latest 33  $H(z)$  measurements (in units of  $\text{km s}^{-1} \text{Mpc}^{-1}$ ) obtained with the differential age method and their associated errors on which we perform our analysis. It is noted that all these measurements are independent, since they come from different datasets.

$z$	$H(z)$	$\sigma_{H(z)}$	Method	Reference
0.07	69	19.6	Full-spectrum fitting	[42]
0.09	69	12	Full-spectrum fitting	[43]
0.12	68.6	26.2	Full-spectrum fitting	[42]
0.17	83	8	Full-spectrum fitting	[43]
0.179	75	4	Calibrated D4000	[44]
0.199	75	5	Calibrated D4000	[44]
0.20	72.9	29.6	Full-spectrum fitting	[42]
0.27	77	14	Full-spectrum fitting	[43]
0.28	88.8	36.6	Full-spectrum fitting	[42]
0.352	83	14	Calibrated D4000	[44]
0.38	83	13.5	Calibrated D4000	[45]
0.4	95	17	Full-spectrum fitting	[43]
0.4004	77	10.2	Calibrated D4000	[45]
0.425	87.1	11.2	Calibrated D4000	[45]
0.445	92.8	12.9	Calibrated D4000	[45]
0.47	89.0	49.6	Full-spectrum fitting	[46]
0.4783	80.9	9	Calibrated D4000	[45]
0.48	97	62	Full-spectrum fitting	[47]
0.593	104	13	Calibrated D4000	[44]
0.68	92	8	Calibrated D4000	[44]
0.75	98.8	33.6	Lick indices	[48]
0.781	105	12	Calibrated D4000	[44]
0.80	113.1	28.5	Full-spectrum fitting	[49]
0.875	125	17	Calibrated D4000	[44]
0.88	90	40	Full-spectrum fitting	[47]
0.9	117	23	Full-spectrum fitting	[43]
1.037	154	20	Calibrated D4000	[44]
1.3	168	17	Full-spectrum fitting	[43]
1.363	160	33.6	Calibrated D4000	[50]
1.43	177	18	Full-spectrum fitting	[43]
1.53	140	14	Full-spectrum fitting	[43]
1.75	202	40	Full-spectrum fitting	[43]
1.965	186.5	50.4	Calibrated D4000	[50]

#### 4. Analysis and Results

To obtain our results, aside from BAO measurements listed in Table 1 done by DESI and DES, we use the Pantheon data given in [40], the latest observational  $H(z)$  measurements using the differential age method containing 33 data points listed in Table 2, and the latest Hubble constant measurement, labeled as R22 [7]. We consider the combination of BAO + OHD + Pantheon datasets as the full dataset.

##### 4.1. Flat $\Lambda$ CDM Model

We present cosmological constraints for the flat  $\Lambda$ CDM model where  $\Omega_k = 0$ ,  $\Omega_\Lambda = 1 - \Omega_m$ . We set  $\Omega_m$ ,  $\Omega_\Lambda$ ,  $H_0$ , and  $r_d$  as free parameters with the following prior:  $\Omega_m \in [0, 1]$ ,  $\Omega_{DE} \in [0, 1 - \Omega_m]$ ,  $H_0$  ( $\text{km s}^{-1} \text{Mpc}^{-1}$ )  $\in [50, 100]$ , and  $r_d$  (Mpc)  $\in [100, 200]$ . The recent measurement of the Hubble constant  $H_0 = 73.04 \pm 1.04 \text{ km s}^{-1} \text{Mpc}^{-1}$  is included into our study as an additional prior, labeled as R22.

In Figure 1 are depicted our results at 68% and 95% confidence levels for the posterior distribution in the  $\Omega_m - \Omega_\Lambda$ ,  $H_0 - \Omega_m$ , and  $r_d - H_0$  and contour planes of the standard model of cosmology  $\Lambda$ CDM. Regarding BAO data alone, the matter density is estimated at 68% C.L.  $\Omega_m = 0.251 \pm 0.030$ , giving a smaller value than the one estimated by *Planck* 2018 [1], but this has been reported in other studies [38,58,59]. The center panel summarizes the constraints in  $\Omega_m - H_0$  plane obtained from the combination of BAO data with R22 prior, and other datasets. All combinations prefer somehow higher values of  $H_0$  and lower ones of matter density  $\Omega_m$  than the ones estimated by *Planck* [1]. However, they fall in the range of agreement with the values estimated by DESI collaboration [38]. In the right panel it is noticed that combining BAO with OHD and Pantheon or with R22 prior, we break the degeneracy in the  $r_d - H_0$  contour plane. The joint analysis of BAO, OHD, and Pantheon, where we refer it as

our full dataset gives the constraint of Hubble constant  $H_0 = 69.65 \pm 1.07 \text{ km s}^{-1} \text{ Mpc}^{-1}$  and sound horizon at the baryon decoupling  $r_d = 147.71 \pm 2.18 \text{ Mpc}$ . By adding Riess 2022 prior for  $H_0$ , the fit gives  $H_0 = 71.55 \pm 0.78 \text{ km s}^{-1} \text{ Mpc}^{-1}$  (which is closer to the value measured by SH0ES team 2022 [7]) and  $r_d = 144.04 \pm 1.58 \text{ Mpc}$ . Ref. [60] finds  $r_d = 143.9 \pm 3.1 \text{ Mpc}$ . Ref. [61] reports that using binning and Gaussian methods to combine measurements of the 2D BAO and SNe data, the values of the absolute BAO scale range from  $141.45 \text{ Mpc} \leq r_d \leq 159.44 \text{ Mpc}$  (binning) and  $143.35 \text{ Mpc} \leq r_d \leq 161.59 \text{ Mpc}$  (Gaussian). The estimation of  $r_d$  with different techniques demonstrate a clear discrepancy between early- and late-time observational measurements, analogously to the  $H_0$  tension. It should be noticed that our results depend on the range of priors for  $r_d$  and  $H_0$ , shifting the estimated values in the  $r_d - H_0$  contour plane. A noticeable feature is that when we do not include the Riess 2022 prior the results of  $H_0$  and  $r_d$  tend to be in agreement with the *Planck* [1].

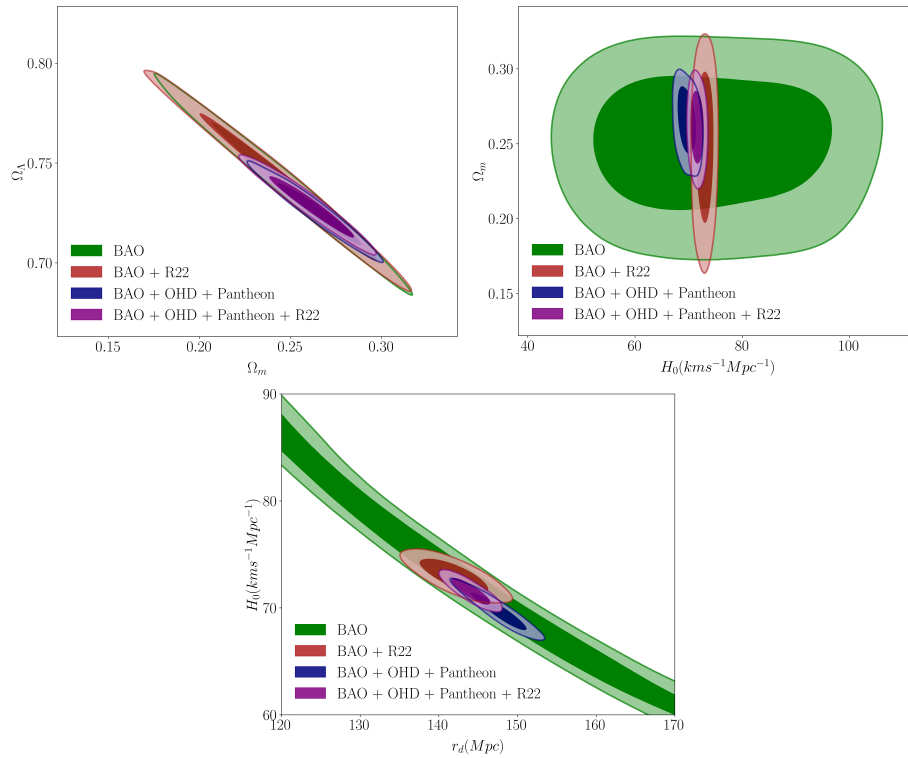


**Figure 1.** Left panel: marginalized posterior cosmic constraints on dark energy parameter density  $\Omega_\Lambda$  and matter density  $\Omega_m$ . Center panel: marginalized posterior cosmic constraints on matter parameter density  $\Omega_m$  and the Hubble constant  $H_0$ , obtained from combining BAO with external data used to calibrate the BAO characteristic scale  $r_d$ . Right panel: marginalized posterior constraints on the sound horizon at the baryon decoupling  $r_d$  and the Hubble constant  $H_0$ , which shows that R22 prior breaks the degeneracy between  $r_d$  and  $H_0$ .

**Table 3.** Mean parameters and constraints values at 68% CL for the standard  $\Lambda$ CDM model based on the BAO measurements listed in Table 1, the observational  $H(z)$  measurements OHD listed in Table 2, Pantheon SNe Ia data [40], and the Gaussian prior R22 [7].

Parameter	BAO + R22	BAO + OHD + Pantheon	BAO + OHD + Pantheon + R22
$H_0$ ( $\text{km s}^{-1} \text{ Mpc}^{-1}$ )	$72.98 \pm 1.07$	$69.65 \pm 1.07$	$71.55 \pm 0.78$
$\Omega_m$	$0.248 \pm 0.033$	$0.265 \pm 0.014$	$0.261 \pm 0.014$
$\Omega_\Lambda$	$0.738 \pm 0.023$	$0.725 \pm 0.010$	$0.728 \pm 0.010$
$r_d$ (Mpc)	$142.00 \pm 2.76$	$147.71 \pm 2.18$	$144.04 \pm 1.58$

#### 4.2. $\Lambda$ CDM Model with Free Curvature

In the  $\Lambda$ CDM model with free spatial curvature, we allow the parameter of curvature  $\Omega_k$  to vary with the prior  $\Omega_k \in [-0.1, 0.1]$  and  $\Omega_m \in [0.1, 1 - \Omega_\Lambda]$ . For the other priors, they are the same as for flat  $\Lambda$ CDM model. In Figure 2 we show the 68% and 95% confidence levels for the posterior distribution of the cosmic parameters of our interest and the mean parameter values and 68% C.L. uncertainties derived from the combinations of data sets are listed in Table 4.

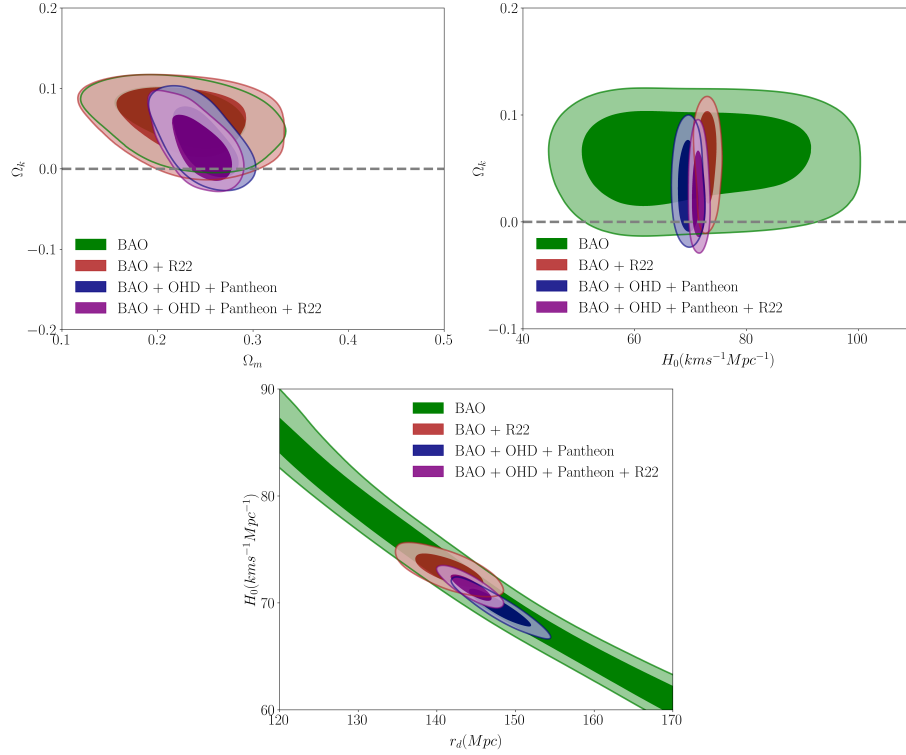


**Figure 2.** Constraints on different cosmic parameters in the  $\Lambda$ CDM model with free spatial curvature. *Left panel:* 68% and 95% marginalized posterior cosmic constraints on  $\Omega_k - \Omega_m$  plane. *Center panel:* 68% and 95% marginalized posterior cosmic constraints on  $\Omega_k - H_0$  plane. *Right panel:* 68% and 95% marginalized posterior constraints on the sound horizon at the baryon decoupling  $r_d$  and the Hubble constant  $H_0$ , which shows that R22 prior breaks the degeneracy between  $r_d$  and  $H_0$ .

**Table 4.** Mean parameters and constraints values at 68% CL for the  $\Lambda$ CDM model with free spatial curvature based on the BAO measurements listed in Table 1, the observational  $H(z)$  measurements OHD listed in Table 2, Pantheon SNe Ia data [40], and the Gaussian prior R22 [7].

Parameter	BAO + R22	BAO + OHD + Pantheon	BAO + OHD + Pantheon + R22
$H_0$ (km s <sup>-1</sup> Mpc <sup>-1</sup> )	73.05 $\pm$ 0.94	69.54 $\pm$ 1.15	71.45 $\pm$ 0.79
$\Omega_m$	0.226 $\pm$ 0.043	0.248 $\pm$ 0.020	0.244 $\pm$ 0.020
$\Omega_\Lambda$	0.696 $\pm$ 0.032	0.707 $\pm$ 0.020	0.716 $\pm$ 0.020
$\Omega_k$	0.061 $\pm$ 0.031	0.032 $\pm$ 0.028	0.025 $\pm$ 0.026
$r_d$ (Mpc)	141.50 $\pm$ 2.76	147.94 $\pm$ 2.54	144.34 $\pm$ 1.65

In this model, for BAO measurements from DESI DR1 and DES Year 6 alone thus measure the parameters ( $\Omega_m$ ,  $\Omega_\Lambda$ ) finding the following 68% constraints values of  $\Omega_m = 0.225 \pm 0.041$ ,  $\Omega_\Lambda = 0.700 \pm 0.032$ . Referring to curvature, we find  $\Omega_k = 0.059 \pm 0.032$ . For the full dataset, we estimate the values of  $H_0$ ,  $r_d$ , and  $\Omega_k$  at  $69.54 \pm 1.15$  km s<sup>-1</sup> Mpc<sup>-1</sup>,  $147.94 \pm 2.54$  Mpc,  $0.032 \pm 0.028$ , respectively. The value of  $\Omega_k$  for all data combinations as listed in Table 4 do not take a negative spatial curvature ( $\Omega_k < 0$ ), which is similar to the DESI result  $\Omega_k = 0.065^{+0.068}_{-0.078}$  [38] and different from the results



obtained by *Planck* for CMB alone [1]. The estimated results are very close to zero so they do not rule out a flat universe.

#### 4.3. Flat $w$ CDM Model

In Figure 3 we show the 68% and 95% confidence levels for the posterior distribution of the cosmic parameters of our interest and the mean parameter values and 68% C.L. uncertainties derived from the combinations of data sets are listed in Table 5.

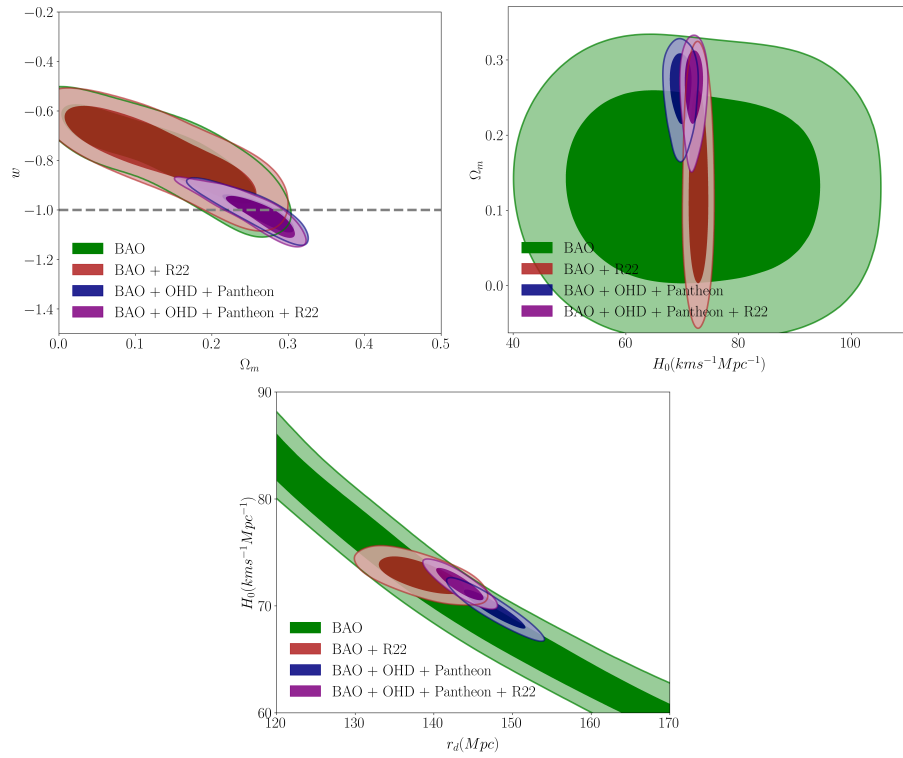


**Figure 3.** Left panel: 68% and 95% marginalized posterior cosmic constraints on  $\Omega_m - w$  plane. Center panel: 68% and 95% marginalized posterior cosmic constraints on  $\Omega_m - H_0$  plane. Right panel: 68% and 95% marginalized posterior constraints on the sound horizon at the baryon decoupling  $r_d$  and the Hubble constant  $H_0$ , which shows that R22 prior breaks the degeneracy between  $r_d$  and  $H_0$ .

**Table 5.** Constraints at 68% CL on the cosmological parameters for the flat constant  $w$ CDM model based on the BAO measurements listed in Table 1, the observational  $H(z)$  measurements OHD listed in Table 2, Pantheon SNe Ia data, and the Gaussian prior R22.

Parameter	BAO + R22	BAO + OHD + Pantheon	BAO + OHD + Pantheon + R22
$H_0$ (km s <sup>-1</sup> Mpc <sup>-1</sup> )	72.83 ± 1.12	69.72 ± 1.14	72.02 ± 0.95
$\Omega_m$	0.130 ± 0.087	0.261 ± 0.032	0.262 ± 0.033
$\Omega_\Lambda$	0.827 ± 0.073	0.727 ± 0.023	0.727 ± 0.023
$w$	-0.766 ± 0.121	-1.006 ± 0.049	-1.016 ± 0.056
$r_d$ (Mpc)	138.30 ± 3.36	147.64 ± 2.50	143.31 ± 1.82

In the left panel of Figure 3 we show the constraints on  $\Omega_m$  and  $w$  derived from the latest DESI and DES BAO measurements and combinations, while in the center and right panel show the corresponding bounds on  $r_d$  and  $H_0$ . In the plane  $\Omega_m - w$  we find for the full dataset  $\Omega_m = 0.261 \pm 0.032$ ,  $w = -1.006 \pm 0.049$ , while combining the full dataset with the R22 prior for  $H_0$  the constraint on  $w$  leads to  $w = -1.016 \pm 0.056$ . Therefore, we observe that the dark energy equation of state we obtain for the full dataset is in agreement with the value estimated by the CMB *Planck* satellite [1] which results  $w = -1.03 \pm 0.03$  and consistent with a cosmological constant. However, when we consider BAO

alone and BAO + R22 the equation of state is  $2\sigma$  away from the cosmological constant, which result  $w = -0.770 \pm 0.120$ ,  $w = -0.766 \pm 0.121$ , respectively. Although these results are obtained in the flat  $w$ CDM model, they are consistent with the results from DESI collaboration [38] when the equation of state is allowed to vary with time  $w(a) = w_0 + (1 - a)w_a$  where DESI data prefer solutions  $w_0 > -1$  and  $w_a < 0$ , but this will require further investigation. Referring to the center and right panel in Figure 3, we observe that the sound horizon at the baryon decoupling  $r_d$  and the Hubble constant  $H_0$  regarding the full dataset tend to be in agreement with the values estimated by *Planck* [1], while combining the full dataset with R22 prior for  $H_0$ , we find  $r_d = 143.31 \pm 1.82$  Mpc, which is consistent with other results [58,60,62].

#### 4.4. Phenomenological Emergent Dark Energy Model

Motivated by the current issues of cosmological observations of the accelerated cosmic expansion, a new model which proposes dark energy with no effective presence in the past and emerging at later times has caught the attention [51]. This dark energy model with zero degrees of freedom (similar to the  $\Lambda$ CDM) is called phenomenological emergent dark energy. We show our results in Figure 4, in which we show the 68% and 95% confidence levels for the posterior distribution of the cosmic parameters of our interest and the mean parameter values and 68% C.L. uncertainties derived from the combinations of data sets are listed in Table 6.

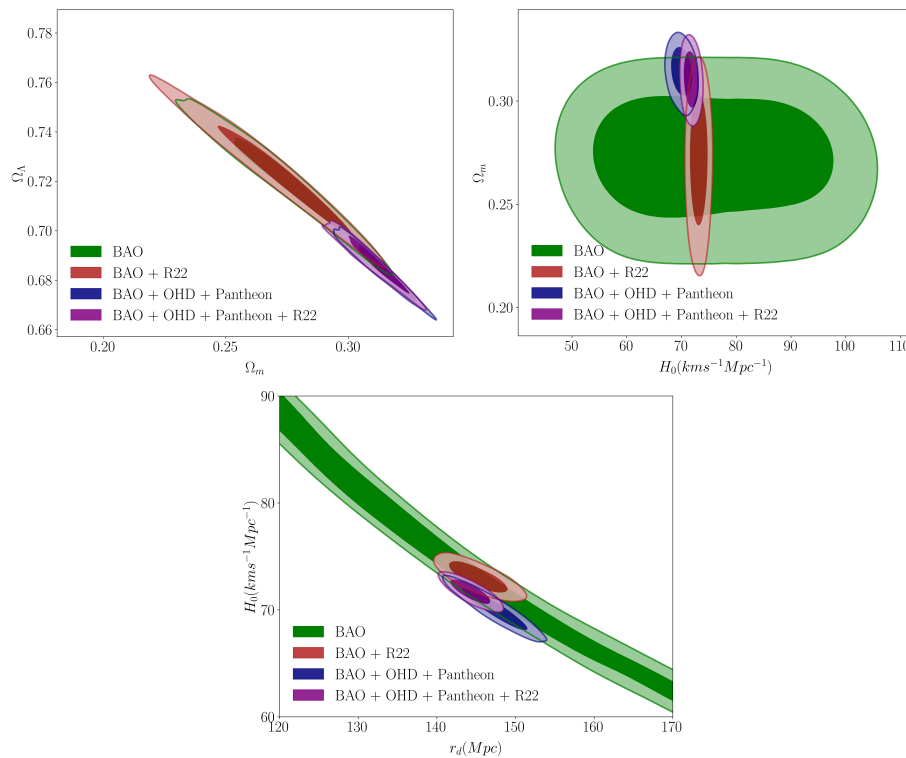


**Figure 4.** Constraints on different cosmic parameters in the PEDE model. *Left panel:* 68% and 95% marginalized posterior cosmic constraints on  $\Omega_\Lambda - \Omega_m$  plane. *Center panel:* 68% and 95% marginalized posterior cosmic constraints on  $\Omega_m - H_0$  plane. *Right panel:* 68% and 95% marginalized posterior constraints on the sound horizon at the baryon decoupling  $r_d$  and the Hubble constant  $H_0$ , which shows that R22 prior breaks the degeneracy between  $r_d$  and  $H_0$ .

**Table 6.** Mean parameters and constraints values at 68% CL for the Phenomenological Emergent Dark Energy (PEDE) model based on the BAO measurements listed in Table 1, the observational  $H(z)$  measurements OHD listed in Table 2, Pantheon SNe Ia data, and the Gaussian prior R22.

Parameter	BAO + R22	BAO + OHD + Pantheon	BAO + OHD + Pantheon + R22
$H_0$ (km s <sup>-1</sup> Mpc <sup>-1</sup> )	73.05 ± 0.96	70.06 ± 1.26	71.75 ± 0.80
$\Omega_m$	0.272 ± 0.018	0.313 ± 0.007	0.310 ± 0.008
$\Omega_\Lambda$	0.722 ± 0.014	0.684 ± 0.007	0.687 ± 0.007
$r_d$ (Mpc)	145.27 ± 2.54	147.39 ± 2.50	145.28 ± 1.73

<sup>1</sup> Tables may have a footer.

In BAO data alone, the matter density parameter results in  $\Omega_m = 0.274 \pm 0.020$ , which is consistent with the value obtained by DESI ( $\Omega_m = 0.295 \pm 0.015$ ) [38]. However, the full dataset gives the value of  $\Omega_m = 0.313 \pm 0.007$  and  $\Omega_\Lambda = 0.684 \pm 0.007$ , which are in excellent agreement with those obtained by *Planck* [1]. Additionally, the Hubble constant is found to be higher at  $H_0 = 70.05 \pm 1.26$  km s<sup>-1</sup> Mpc<sup>-1</sup>, which falls between the *Planck* and SH0ES 2022 measurements of the Hubble constant and is found to be in agreement with measurements from the tip of the red giant branch [31–33]. By incorporating the R22 prior for  $H_0$ , the fit gives a result in accord with the value obtained by SH0ES 2022 [7], while the sound horizon  $r_d$  is in accord with *Planck*:  $H_0 = 71.69 \pm 0.71$  km s<sup>-1</sup> Mpc<sup>-1</sup> and  $r_d = 145.58 \pm 1.60$  Mpc. Additionally, the matter and dark energy densities also are in agreement with the values reported by *Planck* [1], and we do not see a tension in these parameters as it was reported by [51] and with respect to other models studied in this work.

## 5. Discussion

In this work we have provided new measurements on the Hubble constant and sound horizon using the recent BAO measurements from different tracers of the matter density in seven redshift bins performed by the Dark Energy Spectroscopic Instrument DESI year 1 data release [38], the angular diameter distance measurement obtained with the Baryonic Acoustic Oscillation feature from galaxy clustering in the completed Dark Energy Survey, consisting of six years (Y6) of observations [39], the observational  $H(z)$  data, the Pantheon SNe Ia sample, and the R22 prior.

For the full dataset, we determine the Hubble constant and sound horizon values to be  $H_0 = 69.65 \pm 1.07$  km s<sup>-1</sup> Mpc<sup>-1</sup>,  $r_d = 147.71 \pm 2.18$  Mpc<sup>-1</sup> in the standard flat  $\Lambda$ CDM model,  $H_0 = 69.54 \pm 1.15$  km s<sup>-1</sup> Mpc<sup>-1</sup>,  $r_d = 147.94 \pm 2.54$  Mpc<sup>-1</sup> in the  $\Lambda$ CDM+ $\Omega_k$ , and  $H_0 = 69.72 \pm 1.14$  km s<sup>-1</sup> Mpc<sup>-1</sup>,  $r_d = 147.64 \pm 2.50$  Mpc<sup>-1</sup> in the flat  $w$ CDM model. The most interesting results are in the phenomenological emergent dark energy PEDE model: Combining the full dataset with the R22 prior for  $H_0$ , the matter density parameter is  $\Omega_m = 0.310 \pm 0.008$ , the dark energy density parameter  $\Omega_\Lambda = 0.687 \pm 0.007$ , the Hubble constant  $H_0 = 71.89 \pm 0.91$  km s<sup>-1</sup> Mpc<sup>-1</sup>, and the sound horizon  $r_d = 145.28 \pm 1.61$ , reducing or solving the tension from those measured in combination with the CMB full dataset [51]. This is important, as this PEDE model results from our data are in accord with cosmological observations at low [38] and high redshifts [1], and can be a good alternative to explain the effective behavior of dark energy in comparison with the cosmological constant  $\Lambda$ . Of course, this will require detailed studies with more different cosmological observations. To compare our different cosmological models, we use the Akaike information criterion (AIC) and the Bayesian information Criterion (BIC). The AIC criterion is defined as [63]

$$\text{AIC} = -2\ln(\mathcal{L}_{\max}) + 2k + \frac{2k(2k+1)}{N_{\text{tot}} - k - 1}, \quad (9)$$

where  $\mathcal{L}_{\max}$  is the maximum likelihood of the data taken into consideration in which we take the full dataset without the Riess 2022 prior,  $N_{\text{tot}}$  is the total number of data points, and  $k$  is the numbers of parameters. For large  $N_{\text{tot}}$ , our expression is reduced to

$$\text{AIC} \simeq -2\ln(\mathcal{L}_{\max}) + 2k, \quad (10)$$

which is the standard form of the AIC criterion [63]. On the other hand, the Bayesian information criterion is defined as [64]

$$\text{BIC} = -2\ln(\mathcal{L}_{\max}) + k\ln N_{\text{tot}}. \quad (11)$$

Thus, we can calculate the AIC and BIC for the PEDE, standard flat  $\Lambda$ CDM,  $\Lambda$ CDM+ $\Omega_k$ , and flat  $w$ CDM models. We find for the PEDE, standard flat  $\Lambda$ CDM,  $\Lambda$ CDM+ $\Omega_k$ , and flat  $w$ CDM, respectively, AIC = [93.37, 93.84, 95.45, 95.54]. On the other hand, we find for the PEDE, standard flat  $\Lambda$ CDM,  $\Lambda$ CDM+ $\Omega_k$ , and flat  $w$ CDM, respectively, BIC = [94.12, 94.59, 96.61, 96.63]. Our AIC and BIC values suggest that the PEDE model has the best fit in comparison with the other cosmological models studied here. Consequently, making the comparison of our results with other studies, we see that our values are consistent with DESI collaboration official results [38] for the same models studied there by the inclusion of the observation  $H(z)$  measurements (OHD) and R22 prior and the exclusion of the CMB full dataset. As for the PEDE model, the tension remaining in the estimation of the matter density reported in [51] vanishes by incorporating the BAO measurements done by DESI and DES disregarding the CMB full dataset. In conclusion, the BAO information obtained by DESI and DES demonstrates an enormous power for deriving values and constraints of the cosmological parameters when combined with other estimations for the sound horizon and Hubble constant.

**Funding:** This research received no external funding.

**Institutional Review Board Statement:** Not applicable.

**Informed Consent Statement:** Not applicable.

**Data Availability Statement:** The data underlying this article is already given with references during the analysis of this work.

**Acknowledgments:** We would like to thank CONAHCYT for sponsoring this project.

**Conflicts of Interest:** The author declare no conflicts of interest. The funders had no role in the design of the study; in the collection, analyses, or interpretation of data; in the writing of the manuscript; or in the decision to publish the results.

## References

1. Planck Collaboration. Planck 2018 Results—VI. Cosmological Parameters. *Astron. Astrophys.* **2020**, *A6*, 641.
2. Bennett, C.L.; Larson, D.; Weil, J.L.; Jarosik, N.; Hinshaw, G.; Odegard, N.; Smith, K.M.; Hill, R.S.; Gold, B.; Halpern, M.; et al. Nine-year Wilkinson microwave anisotropy probe (WMAP) observations: Final maps and results. *Astrophys. J. Suppl. Ser.* **2013**, *208*, 20.
3. Riess, A.G.; Filippenko, A.V.; Challis, P.; Clocchiatti, A.; Diercks, A.; Garnavich, P.M.; Gillil, R.L.; Hogan, C.J.; Jha, S.; Kirshner, R.P.; et al. Observational Evidence from Supernovae for an Accelerating Universe and a Cosmological Constant. *Astron. J.* **1998**, *116*, 1009.
4. Riess, A.G.; Macri, L.; Casertano, S.; Lampeitl, H.; Ferguson, H.C.; Filippenko, A.V.; Jha, S.W.; Li, W.; Chornock, R. A 3% solution: Determination of the Hubble constant with the Hubble space telescope and wide field camera 3. *Astron. J.* **2011**, *730*, 119.
5. Riess, A.G.; Macri, L.M.; Hoffmann, S.L.; Scolnic, D.; Casertano, S.; Filippenko, A.V.; Tucker, B.E.; Reid, M.J.; Jones, D.O.; Silverman, J.M.; et al. A 2.4% determination of the local value of the Hubble constant. *Astron. J.* **2016**, *826*, 56.
6. Riess, A.G.; Casertano, S.; Yuan, W.; Macri, L.M.; Scolnic, D. Large Magellanic Cloud Cepheid Standards Provide a 1% Foundation for the Determination of the Hubble Constant and Stronger Evidence for Physics beyond  $\Lambda$ CDM. *Astron. J.* **2019**, *876*, 55.
7. Riess, A.G.; Yuan, W.; Macri, L.M.; Scolnic, D.; Brout, D.; Casertano, S.; Jones, D.O.; Murakami, Y.; Anand, G. S.; Breuval, L.; et al. A Comprehensive Measurement of the Local Value of the Hubble Constant with 1 km/s/Mpc Uncertainty from the Hubble Space Telescope and the SH0ES Team. *Astrophys. J. Lett.* **2022**, *934*, L7.
8. Huang, Q.G.; Wang, K. How the dark energy can reconcile Planck with local determination of the Hubble constant. *Eur. Phys. J.* **2016**, *76*, 506.

9. Di Valentino, E.; Melchiorri, A.; Silk, J. Reconciling Planck with the local value of  $H_0$  in extended parameter space. *Phys. Lett. B* **2016**, *761*, 242–246.
10. Xu, L.; Huang, Q.G. Detecting the neutrinos mass hierarchy from cosmological data. *Sci. China Phys. Mech. Astron.* **2018**, *61*, 039521.
11. Yang, W.; Pan, S.; Di Valentino, E.; Saridakis, E.N.; Chakraborty, S. Observational constraints on one-parameter dynamical dark-energy parametrizations and the  $H_0$  tension. *Phys. Rev. D* **2019**, *99*, 043543.
12. Poulin, V.; Smith, T.L.; Karwal, T.; Kamionkowski, M. Early Dark Energy can Resolve the Hubble Tension. *Phys. Rev. Lett.* **2019**, *122*, 221301.
13. Vagnozzi, S. New physics in light of the  $H_0$  tension: An alternative view. *Phys. Rev. D* **2020**, *102*, 023518.
14. Liu, M.; Huang, Z.; Luo, X.; Miao, H.; Singh, N.K.; Huang, L. Can non-standard recombination resolve the Hubble tension? *Sci. China Phys. Mech. Astron.* **2020**, *63*, 290405.
15. Ding, Q.; Nakama, T.; Wang, Y. A gigaparsec-scale local void and the Hubble tension. *Sci. China Phys. Mech. Astron.* **2020**, *63*, 290403.
16. Ryan, J.; Chen, Y.; Ratra, B. Baryon acoustic oscillation, Hubble parameter, and angular size measurement constraints on the Hubble constant, dark energy dynamics, and spatial curvature. *Mon. Not. R. Astron. Soc.* **2019**, *488*, 3844–3856.
17. Zhao, G.B.; Raveri, M.; Pogosian, L.; Wang, Y.; Crittenden, R.G.; H. ley, W.J.; Percival, W.J.; Beutler, F.; Brinkmann, J.; Chuang, C.; et al. Dynamical dark energy in light of the latest observations. *Nat. Astron.* **2017**, *1*, 627–632.
18. Li, X.; Shafieloo, A. A Simple Phenomenological Emergent Dark Energy Model can Resolve the Hubble Tension. *Astrophys. J. Lett.* **2019**, *883*, L3.
19. Di Valentino, E. Investigating Cosmic Discordance. *Astrophys. J. Lett.* **2021**, *908*, L9.
20. Haitao, M.; Zhiqi, H. The  $H_0$  Tension in Non-flat  $\Lambda$ CDM Cosmology. *Astron. J.* **2018**, *868*, 20.
21. Millon, M.; Galan, A.; Courbin, F.; Treu, T.; Suyu, S. H.; Ding, X.; Birrer, S.; Chen, G. C.-F.; Shajib, A. J.; Sluse, D.; et al. An exploration of systematic uncertainties in the inference of  $H_0$  from time-delay cosmography. *Astron. Astrophys.* **2020**, *639*, A101.
22. Wong, K.C.; Suyu, S.H.; Chen, G.C.-F.; Rusu, C.E.; Millon, M.; Sluse, D.; Bonvin, V.; Fassnacht, C.D.; Taubenberger, S.; Auger, M.W.; et al. H0LiCOW—XIII. A 2.4 percent measurement of  $H_0$  from lensed quasars: 5.3 $\sigma$  tension between early- and late-Universe probes. *Mon. Not. R. Astron. Soc.* **2020**, *498*, 1420–1439.
23. Mooley, K.P.; Deller, A.T.; Gottlieb, O.; Nakar, E.; Hallinan, G.; Bourke, S.; Frail, D.A.; Hoeshe, A.; Corsi, A.; Hotokezaka, K. Superluminal motion of a relativistic jet in the neutron-star merger GW170817. *Nature* **2018**, *561*, 355–359.
24. The LIGO Scientific Collaboration and The Virgo Collaboration; The 1M2H Collaboration; The Dark Energy Camera GW-EM Collaboration and the DES Collaboration; The DLT40 Collaboration; The Las Cumbres Observatory Collaboration; The VINROUGE Collaboration; The MASTER Collaboration. A gravitational-wave standard siren measurement of the Hubble constant. *Nature* **2017**, *551*, 85–88.
25. Hotokezaka, K.; Nakar, E.; Gottlieb, O.; Nissanke, S.; Masuda, K.; Hallinan, G.; Mooley, K. P.; Deller, A. T. A Hubble constant measurement from the superluminal motion of the jet in GW170817. *Nat. Astron.* **2019**, *3*, 940–944.
26. Wu, Q.; Zhang, G.-Q.; Wang, F.-Y. An 8 percent determination of the Hubble constant from localized fast radio bursts. *Mon. Not. R. Astron. Soc.: Lett.* **2022**, *515*, L1–L5.
27. James, C.W.; Ghosh, E.M.; Prochaska, J.X.; Bannister, K.W.; Bh, ari, S.; Day, C.K.; Deller, A.T.; Glowacki, M.; Gordon, A.C.; Heintz, K.E.; et al. A measurement of Hubble’s Constant using Fast Radio Bursts. *Mon. Not. R. Astron. Soc.* **2022**, *516*, 4862–4881.
28. Pesce, D.W.; Braatz, J.A.; Reid, M.J.; Riess, A.G.; Scolnic, D.; Condon, J.J.; Gao, F.; Henkel, C.; Impellizzeri, C.M.V.; Kuo, C.Y.; Lo K.Y. The Megamaser Cosmology Project. XIII. Combined Hubble Constant Constraints. *Astrophys. J. Lett.* **2020**, *891*, L1.
29. Reid, J.; Pesce, D.W.; Riess, A.G. An Improved Distance to NGC 4258 and Its Implications for the Hubble Constant. *Astrophys. J. Lett.* **2019**, *886*, L27.
30. Kuo, C.Y.; Braatz, J.A.; Lo K.Y.; Reid, M.J.; Suyu, S.H.; Pesce, D.W.; Condon, J.J.; Henkel, C.; Impellizzeri, C.M.V. The Megamaser Cosmology Project. VI. Observations of NGC 6323. *Astron. J.* **2015**, *800*, 26.



31. Freedman, W.L.; Madore, B.F.; Hatt, D.; Hoyt, T.J.; Jang, I.S.; Beaton, R.L.; Burns, C.R.; Lee, M.G.; Monson, A.J.; Neeley, J.R.; et al. The Carnegie-Chicago Hubble Program. VIII. An Independent Determination of the Hubble Constant Based on the Tip of the Red Giant Branch. *Astron. J.* **2019**, *882*, 34.
32. Freedman, W.L.; Madore, B.F.; Hoyt, T.; Jang, I.S.; Beaton, R.; Lee, M.G.; Monson, A.; Neeley, J.; Jeffrey, R. Calibration of the Tip of the Red Giant Branch. *Astron. J.* **2020**, *891*, 57.
33. Freedman, W.L. Measurements of the Hubble Constant: Tensions in Perspective. *Astron. J.* **2021**, *919*, 16.
34. Addison, G.E.; Watts, D.J.; Bennett, C.L.; Halpern, M.; Hinshaw, G.; Weil, J.L. Elucidating  $\Lambda$ CDM: Impact of Baryon Acoustic Oscillation Measurements on the Hubble Constant Discrepancy. *Astron. J.* **2021**, *853*, 119.
35. Moresco, M.; Amati, L.; Amendola, L.; Birrer, S.; Blakeslee, J.P.; Cantiello, M.; Cimatti, A.; Darling, J.; Valle, M.D.; Fishbach, M.; et al. Unveiling the Universe with emerging cosmological probes. *Living Rev. Relativ.* **2022**, *25*, 6.
36. Ballard, W.; Palmese, A.; Magaña, I.; BenZvi, S.; Moon, J.; Ross, A.J.; Rossi, G.; Aguilar, J.; Ahlen, S.; Blum, R.; et al. A dark siren measurement of the Hubble constant with the LIGO/Virgo gravitational wave event GW190412 and DESI galaxies. *arXiv* **2023**, *2311.13062*.
37. Alfradique, V.; Bom, C.R.; Palmese, A.; Teixeira, G.; Santana-Silva, L.; Drlica-Wagner, A.; Riley, A.H.; Rossi, G.; Martínez-Vázquez, C.E.; Sand, D.J.; et al. A dark siren measurement of the Hubble constant using gravitational wave events from the first three LIGO/Virgo observing runs and DELVE. *Mon. Not. R. Astron. Soc.* **2024**, *528*, 3249–3259.
38. DESI Collaboration. DESI 2024 VI: Cosmological Constraints from the Measurements of Baryon Acoustic Oscillations. *arXiv* **2024**, *2404.03002*.
39. DES Collaboration. Dark Energy Survey: A 2.1% measurement of the angular Baryonic Acoustic Oscillation scale at redshift  $z_{eff} = 0.85$  from the final dataset. *arXiv* **2024**, *2402.10696*.
40. Scolnic, D.M.; Jones, D.O.; Rest, A.; Pan, Y.C.; Chornock, R.; Foley, R.J.; Huber, M.E.; Kessler, R.; Narayan, G.; Riess, A.G.; et al. The Complete Light-curve Sample of Spectroscopically Confirmed SNe Ia from Pan-STARRS1 and Cosmological Constraints from the Combined Pantheon Sample. *Astron. J.* **2018**, *859*, 101.
41. Handley, W.J.; Hobson, M.P.; Lasenby, A.N. POLYCHORD: Nested sampling for cosmology. *Mon. Not. R. Astron. Soc.: Lett.* **2015**, *450*, L61–L65.
42. Cong, Z.; Han, Z.; Shuo, Y.; Siqi, L.; Tong-Jie, Z.; Yan-Chun, S. Four new observational  $H(z)$  data from luminous red galaxies in the Sloan Digital Sky Survey data release seven. *Res. Astron. Astrophys.* **2014**, *14*, 1221.
43. Simon, J.; Verde, L.; Jimenez, R. Constraints on the redshift dependence of the dark energy potential. *Phys. Rev. D* **2005**, *71*, 123001.
44. Moresco, M.; Cimatti, A.; Jimenez, R.; Pozzetti, L.; Zamorani, G.; Bolzonella, M.; Dunlop, J.; Lamareille, F.; Mignoli, M.; Pearce, H.; et al. Improved constraints on the expansion rate of the Universe up to  $z \approx 1.1$  from the spectroscopic evolution of cosmic chronometers. *J. Cosmol. Astropart. Phys.* **2012**, *8*, 6.
45. Moresco, M.; Pozzetti, L.; Cimatti, A.; Jimenez, R.; Maraston, C.; Verde, L.; Thomas, D.; Citro, A.; Tojeiro, R.; Wilkinson, D. A 6 percent measurement of the Hubble parameter at  $z \approx 0.45$ : Direct evidence of the epoch of cosmic re-acceleration. *J. Cosmol. Astropart. Phys.* **2016**, *5*, 14.
46. Ratsimbazafy, A.L.; Loubser, S.I.; Crawford, S.M.; Cress, C.M.; Bassett, B.A.; Nichol, R.C.; Väisänen, P. Age-dating luminous red galaxies observed with the Southern African Large Telescope. *Mon. Not. R. Astron. Soc.* **2017**, *467*, 3239–3254.
47. Stern, D.; Jimenez, R.; Verde, L.; Kamionkowski, M.; Stanford, S.A. Cosmic chronometers: Constraining the equation of state of dark energy. I:  $H(z)$  measurements. *J. Cosmol. Astropart. Phys.* **2010**, *2*, 8.
48. Borghi, N.; Moresco, M.; Cimatti, A. Toward a Better Understanding of Cosmic Chronometers: A New Measurement of  $H(z)$  at  $z \approx 0.7$ . *Astrophys. J. Lett.* **2022**, *928*, L4.
49. Jiao, K.; Borghi, N.; Moresco, M.; Zhang, T.-J. New Observational  $H(z)$  Data from Full-spectrum Fitting of Cosmic Chronometers in the LEGA-C Survey. *Astrophys. J. Suppl. Ser.* **2023**, *265*, 48.
50. Moresco, M. Raising the bar: New constraints on the Hubble parameter with cosmic chronometers at  $z \approx 2$ . *Mon. Not. R. Astron. Soc.: Lett.* **2015**, *450*, L16–L20.
51. Li, X.; Shafieloo, A. A Simple Phenomenological Emergent Dark Energy Model can Resolve the Hubble Tension. *Astrophys. J. Lett.* **2019**, *883*, L3.
52. Linder, E.V. Probing gravitation, dark energy, and acceleration *Phys. Rev. D* **2004**, *70*, 023511.

53. Chevallier, M.; Polarski, D. Accelerating universes with scaling dark matter. *Int. J. Mod. Phys. D* **2001**, *10*, 213–223.
54. Linder, E.V. Exploring the Expansion History of the Universe. *Phys. Rev. Lett.* **2003**, *90*, 091301.
55. Jimenez, R.; Loeb, A. Constraining Cosmological Parameters Based on Relative Galaxy Ages. *Astrophys. J.* **2002**, *573*, 37.
56. Lozano Torres, J.A. Testing Cosmic Acceleration from the Late-Time Universe. *Astronomy* **2023**, *2*, 300–314.
57. Kazantzidis, L.; Perivolaropoulos, L. Evolution of the  $f\sigma_8$  tension with the Planck15/ $\Lambda$ CDM determination and implications for modified gravity theories *Phys. Rev. D* **2018**, *97*, 103503.
58. Nunes, R.C.; Yadav, S.K.; Jesus, J.F.; Bernui, A. Cosmological parameter analyses using transversal BAO data. *Mon. Not. R. Astron. Soc.* **2020**, *497*, 2133–2141.
59. Nunes, R.C.; Bernui, A. BAO signatures in the 2-point angular correlations and the Hubble tension. *Eur. Phys. J. C* **2020**, *80*, 1025.
60. Verde, L.; Bernal, J.L.; Heavens, A.F.; Jimenez, R. The length of the low-redshift standard ruler. *Mon. Not. R. Astron. Soc.* **2017**, *467*, 731–736.
61. Lemos, T.; Ruchika, Carvalho, J.C.; Alcaniz, J. Low-redshift estimates of the absolute scale of baryon acoustic oscillations. *Eur. Phys. J. C* **2023**, *83*, 495.
62. Pogosian, L.; Zhao, G.-B.; Jedamzik, K. Recombination-independent Determination of the Sound Horizon and the Hubble Constant from BAO. *Astrophys. J. Lett.* **2020**, *904*, L7.
63. Akaike, H. A new look at the statistical model identification. *IEEE Trans. Autom. Control.* **1974**, *19*, 716–723.
64. Schwarz, G. Estimating the Dimension of a Model. *Ann. Statist.* **1978**, *6*, 461–464.

**Disclaimer/Publisher’s Note:** The statements, opinions and data contained in all publications are solely those of the individual author(s) and contributor(s) and not of MDPI and/or the editor(s). MDPI and/or the editor(s) disclaim responsibility for any injury to people or property resulting from any ideas, methods, instructions or products referred to in the content.